AJCMI
Avicenna Journal of Clinical Microbiology and Infection
Avicenna J Clin Microbiol Infect, 2022; 9(3):x-x. doi:10.34172/ajcmi.2022.xx
http://ajcmi.umsha.ac.ir

Original Article

Eco-Friendly Synthesis, Characterization, and Antimicrobial Study of Chitosan/Bi (OH)3 Nanocomposites

Fatemeh Mehrabi, Mehdi Ranjbar, Sina Bahraminejad*, Mohammad Hasan Moshafi*

Pharmaceutics Research Center, Institute of Neuropharmacology, Kerman University of Medical Sciences, Kerman, Iran

Article history:
Received: xx Sep. 2022
Accepted: xx Dec. 2022
ePublished: xx Mar. 2022

***Corresponding author:**
Mohammad Hasan Moshafi, Pharm.D, PH.D.;
Email: moshafi14@yahoo.com
Sina Bahraminejad, Pharm.D;
Email: s.bahraminejad@kmu.ac.ir

Abstract

Background: Nowadays, antimicrobial resistance is one of the most important concerns caused by the extensive use of antibiotics. Efforts to find new materials with antimicrobial effects have been continued more seriously than before. Nanoparticles (NPs) with very small dimensions and extraordinary properties have the potential to overcome antimicrobial resistance, so the use of previous antimicrobial substances at the nanometer dimensions to investigate physicochemical and antimicrobial effects could help overcome these universal concerns.

Methods: In this study, NPs were synthesized by hydrothermal-assisted microwave technique. Scanning electron microscopy (SEM), dynamic light scattering (DLS), and atomic force microscopy (AFM) were carried out to investigate the physicochemical properties. Further, energy dispersive spectroscopy and Fourier-transform infrared spectroscopy analyses were carried out to analyze the chemical composition of nanocomposites. Then, their minimum inhibitory concentration was measured on seven bacterial isolates.

Results: The majority of NPs were in the range of 40-100 nanometers which is the well-optimized size for our purpose. Antimicrobial analysis revealed the effect of synthesized nanocomposites on every seven microbial isolates, including three gram-positive isolates (i.e., *Staphylococcus aureus, Micrococcus luteus, Bacillus subtilis*) and four gram-negative isolates (i.e., *Serratia marcescens, Escherichia coli, Pseudomonas aeruginosa, Klebsiella pneumoniae*).

Conclusion: Synthesized nanocomposite revealed a good antimicrobial effect on all bacterial isolates. It is suggested to investigate the cellular toxicity of synthesized nanocomposite in the next studies.

Keywords: Microbial resistance, Antibacterial, Bismuth hydroxide/chitosan, Nanocomposite

Please cite this article as follows: Mehrabi F, Ranjbar M, Bahraminejad S, Moshafi MH. Eco-friendly synthesis, characterization, and antimicrobial study of chitosan/bi (OH)3 nanocomposites. Avicenna J Clin Microbiol Infect. 2022; 9(3):x-x. doi:10.34172/ajcmi.2022.xx

Background

In recent years, nanotechnology and nanoengineering have begun to make significant changes in various sciences, especially in the medical field. It can be broadly stated that the science and engineering of design, fabrication, characterization, and application of materials and devices are defined as nanotechnology with particles ranging in size from a few nanometers to hundreds of nanometers. In the general sense, particles ranging from 1 to 100 nm are called nanoparticles (NPs). These particles are designed to exhibit special and controlled properties of their raw material in normal size, which is the result of precise control over their manufacturing process. Nanomedicine is a growing branch of nanotechnology and pharmaceuticals with the goal of expanding drugs, antimicrobials, as well as imaging agents, and today, a highly active branch of science is reducing toxicity profiles. One of the most important aspects of drug delivery systems and pharmaceutics is to constantly improve drug targeting for specific cells and reduce the accumulation of drugs in cells that do not need them, and their presence in those cells has potentially toxic effects on the cells. This is often because the size of the drug molecules that are commonly used is 10 times greater than the size of a cell such as a red blood cell, causing the drug to penetrate the cells much less than expected. As a result, to achieve the desired goals, the dose or frequency of use has to be increased, which in turn causes more toxicity and unwanted side effects (1,2). On the other hand, in the treatment of infectious diseases, bacterial resistance to newer antibiotics has always been and will be an important issue because bacterial resistance leads to increased doses of antibiotics, hospital stay, antimicrobial therapy, and ultimately increased patient mortality (3). Bacteria may be resistant to a group of antibacterial agents inherently or by mutations or by obtaining resistance genes from other organisms. Obtaining resistance genes from resistant bacteria may be achieved by conjugation, bacteriophage transmission, and transfection (4). The sudden and global growth of multidrug-resistant

bacteria has dramatically reduced the effectiveness of new antimicrobials and disrupted the healing process. Despite this spread of resistance among bacteria, the need for innovation in the production of antimicrobials seems undeniable (5). Many investigations have reported the effectiveness of bismuth compounds in preventing diarrhea, especially for *Salmonella*, *Escherichia coli*, and *Shigella* species and in treating acute diarrhea caused by rotavirus and endotoxins. These compounds have also been approved as a supplement in the treatment of gastric and duodenal ulcers caused by *Helicobacter pylori* and the treatment of syphilis, skin infections, and gastrointestinal ulcers such as gastric and duodenal ulcers (6-10). Chitosan is a biodegradable polymer with high biocompatibility, which is non-antigenic and non-toxic. It is abundantly found in oysters, crabs, shrimp, and other marine crustaceans and has many biological benefits. The first mechanism for the antimicrobial effects of chitosan is its ability to form a biofilm and block the oxygen needed for the microorganism to grow, which ultimately leads to the death of the microorganism. In previous studies, various factors have been considered to affect the antimicrobial properties of chitosan, including the type of chitosan and its chain length. It has also been demonstrated that the shorter the chitosan chain length is, the greater its ability will be at penetrating microorganisms, binding to DNA, and preventing mRNA production (11,12). After the fabrication and assessment of the physicochemical properties of bismuth hydroxide/chitosan NPs, this study investigated their antimicrobial effects on seven microbial isolates including *Staphylococcus aureus, Micrococcus luteus, Bacillus subtilis, Serratia marcescens, E. coli, Pseudomonas aeruginosa,* and *Klebsiella pneumoniae*. In the case of antimicrobial effects, the lowest inhibitory concentration for the mentioned isolates was determined.

Materials and Methods

Chitosan NP Synthesis

This study used the chitosan of a non-animal origin with high purity and an average molecular weight of 100 kDa. First, 0.05 grams of chitosan was weighed, and then 15 mL of a 2:1 solution of water and ethanol was added and dissolved well by slow stirring. After dissolving the chitosan, the mixture was placed on a heater stirrer at 50˚C and 400 rpm for 30 minutes to remove the organic solvent from the system. Then, adjusting the PH was conducted by adding 5 mL of sodium hydroxide 2 M to the reaction medium. Finally, the electrostatic atmosphere of the ions was stabilized by 5 mg of sodium dodecyl sulfate. This operation was repeated for 0.1 g and 1 g of chitosan. At this pH, the concentration of OH ions is such that during the nucleation process, hydrogen bonds are easily formed between the chitosan polymers, thus preventing the polymers from squeezing together (13,14).

Synthesis of Bi(OH)3 Nanostructures

Briefly, 20 mL of 0.1% w/w bismuth nitrate was added to 10 mL of 2:1 solution of water and ethanol and stirred well at 50˚C and 400 rpm for 30 minutes in a reflux system in order to remove the organic solvent. The resulting mixture was then placed in the reflux system for 45 minutes. During this period, 15 mL of NaOH 2 M was added drop by drop to the mixture. This process was associated with discoloration due to the formation of primary nuclei of NPs. During this process, bismuth nitrate was converted to bismuth hydroxide in the presence of hydroxide ions. This operation was repeated for 0.5% and 1% w/w bismuth nitrate. After that, the prepared mixtures were put in a microwave. For this purpose, 0.5%, 0.1%, and 1% w/w bismuth hydroxide were placed in a microwave at 600, 750, and 900 W for 15 minutes, respectively, with specific nucleation and growth on and off cycles (14,15).

Chitosan/Bi(OH)3 Nanocomposites

Nanocomposites with three different concentrations were synthesized as follows:

- A sample containing 0.1% w/w chitosan was added to 0.1% w/w bismuth hydroxide (nanocomposites A).
- A sample containing 0.5% w/w chitosan was added to 0.5% w/w bismuth hydroxide (nanocomposites B).
- A sample containing 1% w/w chitosan was added to 1% w/w bismuth hydroxide (nanocomposites C).

Accordingly, all three final compounds were separately heated at 50 ˚C and 400 rpm for 50 minutes by a heater and then located in a microwave at 180˚C for 5 minutes.

Antimicrobial Assay

In this study, evaluation of the antimicrobial activity of the fabricated nanocomposites was carried out by measuring the minimum inhibitory concentration of each nanocomposite for seven microbial isolates according to the Clinical and Laboratory Standards Institute (16).

Results

Characterization of Chitosan/Bi(OH)3 Nanostructures

Scanning electron microscopy (SEM) was used to assess the shape and size of chitosan/$Bi(OH)_3$ NPs. The outcomes of SEM images for the chitosan/$Bi(OH)_3$ nanocomposites related to samples a, b, and c are presented in Figures 1a, 1b, and 1c, respectively (200 nm magnification). Uniform dispersion and agglomerated zone can be observed in SEM images of chitosan structures. Moreover, the relative small sizes of chitosan/$Bi(OH)_3$ NPs with a uniform spherical shape were observed.

In the present study, the dynamic light scattering (DLS) method was employed to measure the hydrodynamic diameter. The particle size at 25˚C, 0.1 mL of chitosan/$Bi(OH)_3$ NP solution in 2 mL of deionized water was calculated using a polystyrene cuvette. Figure 2 exhibits the size distribution by the intensity of chitosan/$Bi(OH)_3$ NPs of sample A. The size of the chitosan/$Bi(OH)_3$ NPs of samples A, B, and C was calculated to be approximately 297, 475, and 578 nm, respectively. According to the DLS data analysis of sample A, Dn 10%: 71.02 nm, Dn

50%: 342.09 nm, and Dn 90%: 543.17 nm were obtained. Furthermore, Dn 10%: 112.77 nm, Dn 50%: 518.63 nm, and Dn 90%: 543.17 nm were acquired for sample B, and Dn 10%: 568.88 nm, Dn 50%: 595.8 nm, and Dn 90%: 623.99 nm were estimated for sample C.

The chemical composition and functional groups of chitosan/$Bi(OH)_3$ NPs were identified using Fourier transform infrared (FT-IR) spectroscopy as a non-destructive technique. As can be found in Figure 3, the FT-IR results were evaluated in the range from 500 cm^{-1} to 3500 cm^{-1}. The sharpest peaks were observed at 618, 1138, 1492, 1630, 2850, 2922, and 3422 cm^{-1} regions for all three samples of nanocomposites.

The peaks illustrated at 1138, 1492, and 2850 cm^{-1} were related to the C-O, C-N, and C-H functional groups in chitosan polymers, and the peaks at 2922 and 3422 cm^{-1} were related to the C-H, N-H, and O-H functional groups in chitosan polymers. The peak at 1660 cm^{-1} indicated the formation of an imine bond between the chitosan and bismuth hydroxide groups (C=N) and the 618 cm^{-1} peak belonged to the Bi-O functional group after cross-linking between the chitosan and bismuth molecules.

Figure 4 depicts the results of the ultraviolet analysis of chitosan/$Bi(OH)_3$ NPs. The first peak was observed at a wavelength between 200 and 205 nm related to chitosan NPs as expected, and the maximum absorption belonged to a wavelength of 260 nm.

Figure 5 indicates that the evaluation of the crystalline properties of chitosan/$Bi(OH)_3$ NPs was performed by X-ray powder diffraction analysis. Given that all samples had the same precursor, similar results were obtained. Examination of the X-ray pattern of the sample revealed that the structure follows a hexagonal pattern, and a crystalline structure is formed in it.

As Table 1 illustrates, energy dispersive X-ray (EDX) was employed to acquire the accurate percentage of elements in the final samples. EDX assay is a nondestructive method for the chitosan/$Bi(OH)_3$ NPs samples.

The highest mass percentage of elements belonged to carbon followed by bismuth, which was the main elements of the composition. Nitrogen and sodium impurities were also present in the composition, which were predictable

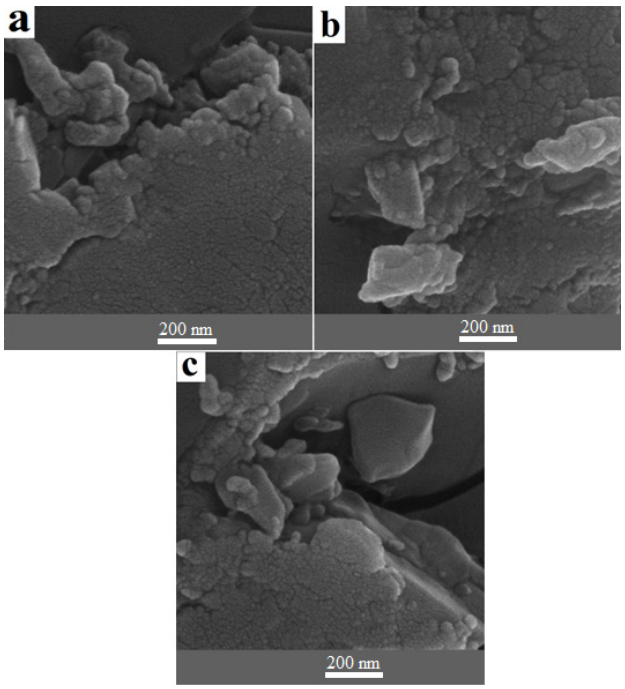

Figure 1. SEM Images of Chitosan/Bi(OH)3 NPs of Sample A (a), Sample B (b), Sample C (c). *Note.* SEM: Scanning electron microscopy; NPS: Nanoparticles

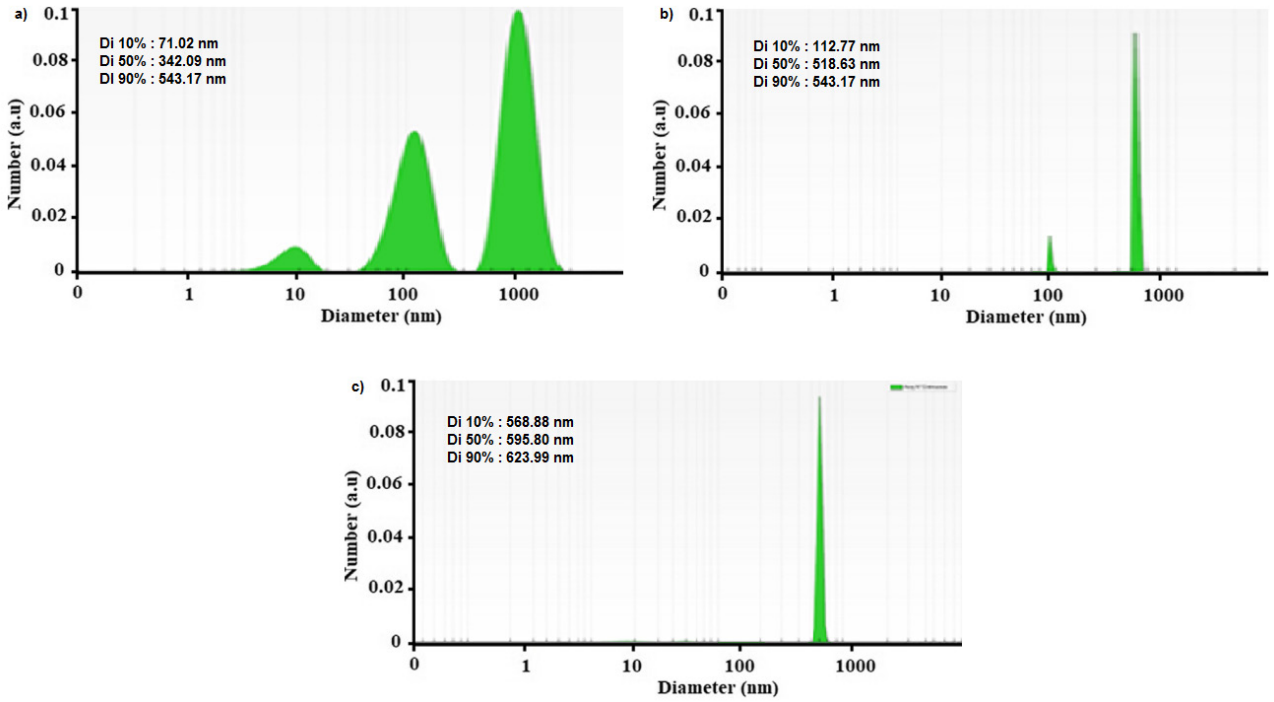

Figure 2. DLS Data Diagram of Chitosan/Bi(OH)3 NPs of Sample A (a), Sample B (b), Sample C (c). *Note.* DLS: Dynamic light scattering; NPs: Nanoparticles

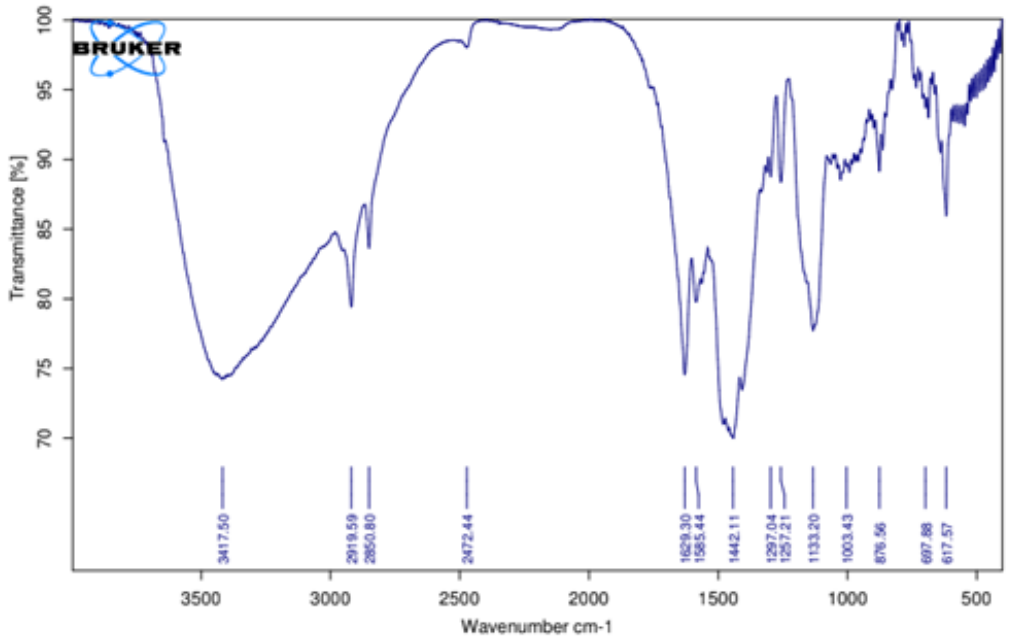

Figure 3. The FT-IR Analysis in the Range of 500 cm-1 up to 3500 cm-1 for Chitosan/Bi(OH)3 NPs. *Note.* FT-IR: Fourier transform infrared; NPs: Nanoparticles

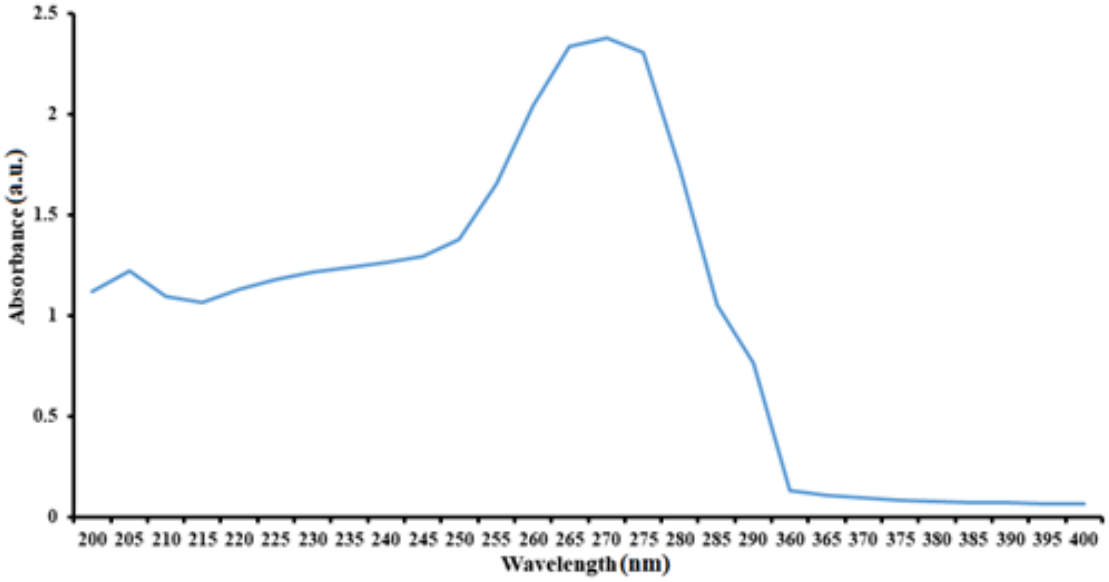

Figure 4. Ultraviolet Spectrum of Chitosan/Bi(OH)3 NPs at the Wavelength Range Between 200-400 nm

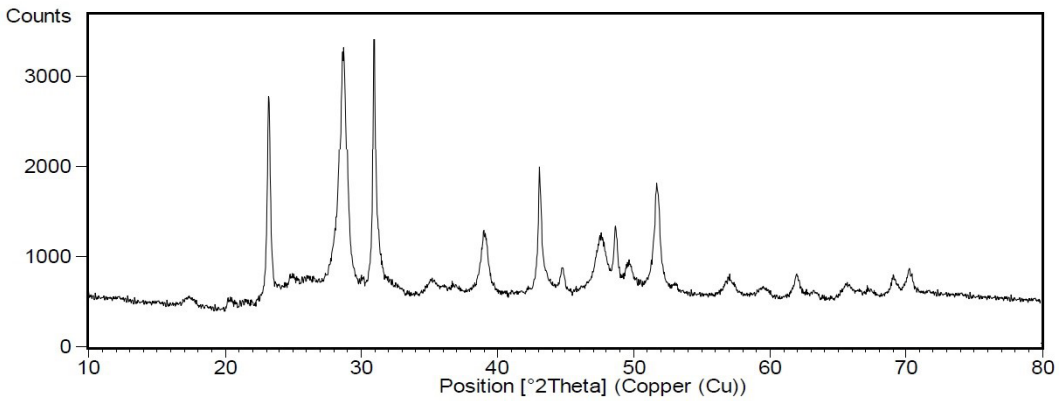

Figure 5. XRD Analysis of the Chitosan/Bi(OH)3 NPs. *Note.* XRD: X-ray powder diffraction; NPs: Nanoparticles

due to the nanoparticle manufacturing process. Two other unwanted impurities were titanium and zinc, which were present in small amounts in the synthesized compound. The presence of titanium could be justified according to the material of the titanium lever of the electron beam transmitter in the device.

Atomic force microscopy (AFM) analysis was performed for NPs of sample A, which had the best particle size and particle size distribution in X-ray diffraction and electron microscopy images. According to Figure 6, the particles had the highest dispersion in the particle size range between 40-100 nm.

Table 2 indicates the minimum concentration inhibiting the growth of the prepared chitosan/$Bi(OH)_3$ NP sample A. As observed in Table 2, all NPs in A, B, and C showed antimicrobial effects on all seven bacterial isolates and prevented the growth of bacterial colonies.

Figure 7 presents the comparison of the antimicrobial effects of all three synthesized nanocomposites.

Table 1. EDX Analysis of Chitosan/Bi(OH)3 NPs

Elt	Line	Int	Error	K	Kr	W%	A%
Bi	Ka	12.9	89.7507	0.0907	0.0798	12.87	43.91
C	Ka	30.9	2.1054	0.6920	0.6080	69.84	28.36
N	Ka	4.9	0.5420	0.0687	0.0605	6.17	12.78
Na	Ka	0.9	0.7098	0.0848	0.0746	6.29	7.98
Zn	Ka	0.8	0.7098	0.0443	0.0390	3.24	4.58
Tl	Ka	0.7	0.3290	0.0194	0.0171	1.58	2.39
Total				1.0000	0.8798	100.00	100.00

Note. EDX: Energy dispersive X-ray; NPs: Nanoparticles. A%: Percentage of atomic mass of elements. W%: Weight percentage of each element.

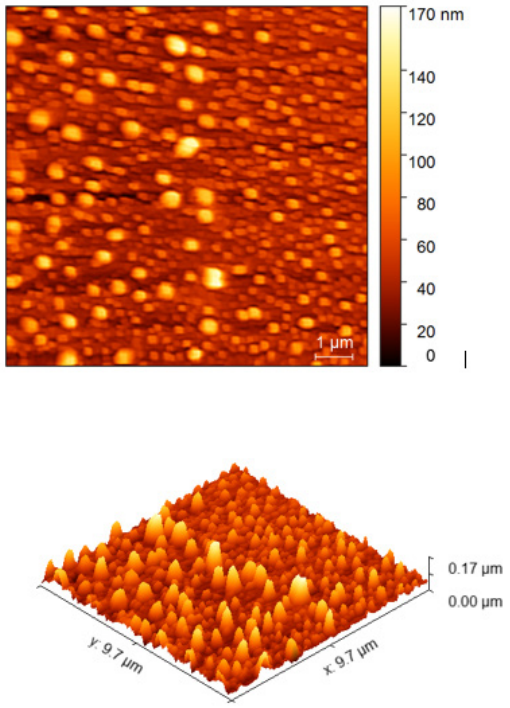

Figure 6. AFM Analysis of Chitosan/Bi(OH)3 NPs. *Note.* AFM: Atomic force microscopy; NPs: Nanoparticles

Discussion

Green synthesis of NPs is an eco-friendly approach that might pave the way for researchers around the world to discover the potential of different bacteria, fungi, yeasts, viruses, algae, plants, plant extracts, fungi, algae, and flower extracts to synthesize NPs (17). Many important properties of NPs depend entirely on their particle size. Characteristics such as the dissolution rate, melting point, and surface-to-volume ratio, which influence intermolecular interactions, significantly affect the antimicrobial properties of the material. Therefore, it is crucial to accurately study the particle size of NPs using the appropriate methods.

According to previous studies, bismuth NPs were expected to have significant absorption at 250 to 280 wavelengths. Studies have also revealed that NPs with a size of 10 nm exhibit maximum absorption at 270 nm (18,19).

In the DLS method, the particle size is generally found to be larger than what it actually is. This is due to the fact that the mechanism of this measurement is the placement of particles under random Brownian motions. Therefore, changes in the index of light reflection and any deviation of the shape of the particles from the spherical state easily lead to large changes in the obtained size. However, this error can be corrected by SEM and AFM. Previous research has demonstrated that although AFM cannot be used to measure every sample, its results are closer to the actual value.

Considering that almost all three particles exhibited the same particle size in the electron microscope image, using the results of X-ray diffraction analysis, the best particle size distribution of NPs was observed in sample A, and thus, it was sent for AFM analysis. As expected, the maximum particle dispersion was between 40 and 100 nm, and the lowest particle dispersion was at 170 nm.

In general, it can be concluded that the combination of hydrothermal and microwave methods for optimizing NPs is ideal because not only did the dimensions of the NPs exactly match what was expected, but the number of impurities in the synthesized NPs was as low as possible according to the EDX analysis.

Regarding the mechanism of antibacterial effects of chitosan, three possible mechanisms are considered. The first one is that it inhibits the growth of gram-positive and gram-negative bacteria by collapsing and altering the permeability of cell walls and membranes. The second mechanism is mediated by inhibiting the transcription of DNA, and in the case of aerobic bacteria, the role of chitosan in masking and preventing the penetration of oxygen into the bacteria can also be one of the possible mechanisms (18). Regarding the first mechanism, the role of the free amine group is considered effective. However, according to the FT-IR spectrum of the composition and what we expected, the free amine is converted to an imine in the synthesized nanocomposites. To justify this, the findings of a study conducted in 2016 can be considered.

Table 2. Minimum Concentration Inhibiting the Growth of Prepared Chitosan/Bi(OH)3 NPs for Sample A

Bacteria	Concentration (µg/mL)												
	64	32	16	8	4	2	1	0.5	0.25	0.125	0.0625	0.03125	0.01562
Escherichia coli PTCC 1330	-	-	-	-	-	-	-	-	+	+	+	+	+
Klebsiella pneumoniae PTCC 1053	-	-	-	-	-	-	-	+	+	+	+	+	+
Serratia marcescens PTCC 1621	-	-	-	-	-	-	-	-	-	+	+	+	+
Bacillus subtilis PTCC 1023	-	-	-	-	-	-	-	-	+	+	+	+	+
Micrococcus luteus OTCC 1110	-	-	-	-	+	+	+	+	+	+	+	+	+
Staphylococcus aureus PTCC 1112	-	-	-	-	-	-	-	+	+	+	+	+	+
Pseudomonas aeruginosa PTCC 1074	-	-	-	-	-	+	+	+	+	+	+	+	+
Positive control	+	+	+	+	+	+	+	+	+	+	+	+	+
Negative control	-	-	-	-	-	-	-	-	-	-	-	-	-

Note. NPs: Nanoparticles. Plus sign shows bacterial growth and minus sign shows no bacterial growth.

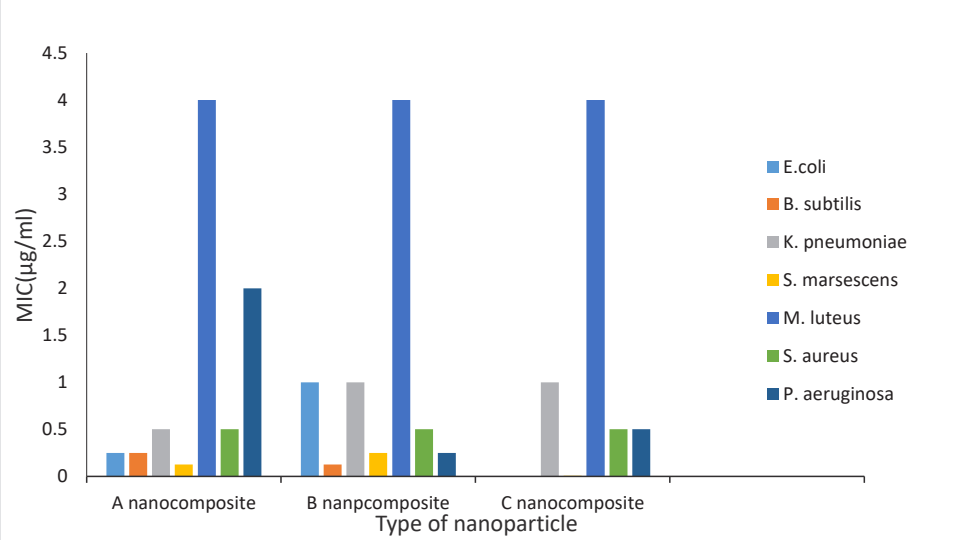

Figure 7. Comparison of Antimicrobial Effects of All Three Synthesized Nanocomposites

In this study, it was observed that by converting the amine group to imine, this effect was not decreased but rather increased. Finally, it is well established that the mechanism of the antimicrobial effect of chitosan is not known yet, but at pH above pKa, it is likely to exert the greatest effect on microorganisms through high hydrophobicity and chelation. However, it is generally believed that the antimicrobial effects of chitosan are the result of a series of sequential reactions rather than a single one (20-22). Previous studies have also evidenced that reducing the size of the chitosan polymer increases its antimicrobial effects because the penetration of chitosan into the microorganism increases. In addition, due to the antioxidant activity and immune-stimulating properties of nano-chitosans, these NPs exhibited antimicrobial effects on a variety of microorganisms; therefore, they are added to other antimicrobial agents to enhance resistance to microbial infections (23,24).

Despite extensive studies on the role of bismuth compounds in the prevention and treatment of diarrhea, there are still controversies regarding the mechanism of action of bismuth. Some studies have indicated that bismuth compounds inhibit small intestinal secretions caused by *Vibrio cholerae* and *E. coli* endotoxins and reduce cellular attacks. In addition, bismuth compounds reduce *K. pneumoniae* attacks. A study has also demonstrated that bismuth inhibits the Rho protein of *E. coli*, a vital protein for controlling the expression of gram-negative bacterial genes. Thus, it can be concluded that the antibacterial properties of bismuth result from multiple mechanisms (25-27). Recently, novel therapeutic strategies have focused on combination of therapies to fight multi-drug resistance organisms (28,29). The present study focused primarily on using non-antibiotic compounds as novel antibiotic agents with different pathways and evaluated their benefits in developing the next generation of combinational therapies. Although several studies separately displayed the antimicrobial activity of bismuth NPs and chitosan NPs against bacteria, fungi, and protozoan, to the best of our knowledge, there is no reported study investigating the antimicrobial effects of chitosan/$Bi(OH)_3$ nanocomposites against these microbial isolates (30-32).

Evidence also suggests that the antibacterial effects of

chitosan reduced in the presence of sodium ions and in basic pH, which can be used in future studies to boost these effects in order to control the sodium content of the product (33). Generally, the antimicrobial properties of the synthesized NPs are very promising.

Conclusion

The present study demonstrates that the minimal inhibitory concentration (MIC) of all NPs was less than 0.5 mg/mL for *B. subtilis*, *E. coli*, and *S. aureus* isolates. Despite slight differences in the particle dispersion of the synthesized NPs, the effect on bacterial isolates was not significantly different between the three synthesized NPs, and in all cases, the highest effect was observed on *S. marcescens* and the least effect was on *M. luteus*. It should be noted that the effectiveness of these NPs on other bacterial isolates due to their low MIC can be considered for future studies. It is also suggested that cytotoxicity be assessed in future research. Moreover, in the synthesis of the compound, it should be attempted to reduce the impurities as much as possible, minimize the amount of sodium in the composition, and test the antimicrobial effects of the synthesized compound under new conditions.

Acknowledgments

The authors are grateful to the council of Pharmaceutics Research Center, Institute of Neuropharmacology, Kerman University of Medical Sciences, Kerman, Iran.

Conflict of Interests

The authors declare that they have no conflict of interests.

Ethical Approval

xxx .

References

1. Yadav N. Application of nanotechnology in health sciences. Plant Arch. 2017;17(1):539-45.
2. Bobo D, Robinson KJ, Islam J, Thurecht KJ, Corrie SR. Nanoparticle-based medicines: a review of FDA-approved materials and clinical trials to date. Pharm Res. 2016;33(10):2373-87. doi: 10.1007/s11095-016-1958-5.
3. Pelgrift RY, Friedman AJ. Nanotechnology as a therapeutic tool to combat microbial resistance. Adv Drug Deliv Rev. 2013;65(13-14):1803-15. doi: 10.1016/j.addr.2013.07.011.
4. Tenover FC. Mechanisms of antimicrobial resistance in bacteria. Am J Med. 2006;119(6 Suppl 1):S3-10; discussion S62-70. doi: 10.1016/j.amjmed.2006.03.011.
5. Djeussi DE, Noumedem JA, Seukep JA, Fankam AG, Voukeng IK, Tankeo SB, et al. Antibacterial activities of selected edible plants extracts against multidrug-resistant Gram-negative bacteria. BMC Complement Altern Med. 2013;13:164. doi: 10.1186/1472-6882-13-164.
6. Gorbach SL. Bismuth therapy in gastrointestinal diseases. Gastroenterology. 1990;99(3):863-75. doi: 10.1016/0016-5085(90)90983-8.
7. DuPont HL, Ericsson CD, Johnson PC, Bitsura JA, DuPont MW, de la Cabada FJ. Prevention of travelers' diarrhea by the tablet formulation of bismuth subsalicylate. JAMA. 1987;257(10):1347-50.
8. Soriano-Brücher H, Avendaño P, O'Ryan M, Braun SD, Manhart MD, Balm TK, et al. Bismuth subsalicylate in the treatment of acute diarrhea in children: a clinical study. Pediatrics. 1991;87(1):18-27.
9. Figueroa-Quintanilla D, Salazar-Lindo E, Sack RB, León-Barúa R, Sarabia-Arce S, Campos-Sánchez M, et al. A controlled trial of bismuth subsalicylate in infants with acute watery diarrheal disease. N Engl J Med. 1993;328(23):1653-8. doi: 10.1056/nejm199306103282301.
10. Steffen R, DuPont HL, Heusser R, Helminger A, Witassek F, Manhart MD, et al. Prevention of traveler's diarrhea by the tablet form of bismuth subsalicylate. Antimicrob Agents Chemother. 1986;29(4):625-7. doi: 10.1128/aac.29.4.625.
11. Kong M, Chen XG, Xing K, Park HJ. Antimicrobial properties of chitosan and mode of action: a state of the art review. Int J Food Microbiol. 2010;144(1):51-63. doi: 10.1016/j.ijfoodmicro.2010.09.012.
12. Agnihotri SA, Mallikarjuna NN, Aminabhavi TM. Recent advances on chitosan-based micro- and nanoparticles in drug delivery. J Control Release. 2004;100(1):5-28. doi: 10.1016/j.jconrel.2004.08.010.
13. Zhao XY, Zhu YJ, Qi C, Chen F, Lu BQ, Zhao J, et al. Hierarchical hollow hydroxyapatite microspheres: microwave-assisted rapid synthesis by using pyridoxal-5′-phosphate as a phosphorus source and application in drug delivery. Chem Asian J. 2013;8(6):1313-20. doi: 10.1002/asia.201300142.
14. Bhuvaneswari T, Thiyagarajan M, Geetha N, Venkatachalam P. Bioactive compound loaded stable silver nanoparticle synthesis from microwave irradiated aqueous extracellular leaf extracts of *Naringi crenulata* and its wound healing activity in experimental rat model. Acta Trop. 2014;135:55-61. doi: 10.1016/j.actatropica.2014.03.009.
15. Khazaeli P, Alaei M, Khaksarihadad M, Ranjbar M. Preparation of PLA/chitosan nanoscaffolds containing cod liver oil and experimental diabetic wound healing in male rats study. J Nanobiotechnology. 2020;18(1):176. doi: 10.1186/s12951-020-00737-9.
16. Humphries R, Bobenchik AM, Hindler JA, Schuetz AN. Overview of Changes to the Clinical and Laboratory Standards Institute Performance Standards for Antimicrobial Susceptibility Testing, M100, 31st Edition. J Clin Microbiol. 2021;59(12):e0021321. doi: 10.1128/jcm.00213-21.
17. Savithramma N, Rao ML, Devi PS. Evaluation of antibacterial efficacy of biologically synthesized silver nanoparticles using stem barks of *Boswellia ovalifoliolata* Bal. and Henry and *Shorea tumbuggaia* Roxb. J Biol Sci. 2011;11(1):39-45. doi: 10.3923/jbs.2011.39.45.
18. Mohammadi M, Tavajjohi A, Ziashahabi A, Pournoori N, Muhammadnejad S, Delavari H, et al. Toxicity, morphological and structural properties of chitosan-coated Bi2O3–Bi (OH) 3 nanoparticles prepared via DC arc discharge in liquid: a potential nanoparticle-based CT contrast agent. Micro Nano Lett. 2019;14(3):239-44. doi: 10.1049/mnl.2018.5145.
19. Fang J, Stokes KL, Zhou WL, Wiemann JA, Dai J, Oconnor CJ. Colloidal bismuth nanoparticles: synthesis and UV-Vis absorption. In: Cluster and Nanostructure Interfaces. World Scientific; 2000. p. 91-6.
20. Liu D, Wei Y, Yao P, Jiang L. Determination of the degree of acetylation of chitosan by UV spectrophotometry using dual standards. Carbohydr Res. 2006;341(6):782-5. doi: 10.1016/j.carres.2006.01.008.
21. Andres Y, Giraud L, Gerente C, Le Cloirec P. Antibacterial effects of chitosan powder: mechanisms of action. Environ Technol. 2007;28(12):1357-63. doi: 10.1080/09593332808618893.
22. Ameri A, Khodarahmi G, Hassanzadeh F, Forootanfar H, Hakimelahi GH. Novel aldimine-type schiff bases of 4-amino-5-[(3,4,5-trimethoxyphenyl)methyl]-1,2,4-triazole-3-thione/thiol: docking study, synthesis, biological evaluation, and anti-tubulin activity. Arch Pharm (Weinheim). 2016;349(8):662-81. doi: 10.1002/ardp.201600021.

23. Akbari M, Oryan A, Hatam G. Application of nanotechnology in treatment of leishmaniasis: a review. Acta Trop. 2017;172:86-90. doi: 10.1016/j.actatropica.2017.04.029.
24. Bahraminegad S, Pardakhty A, Sharifi I, Ranjbar M. The assessment of apoptosis, toxicity effects and anti-leishmanial study of Chitosan/CdO core-shell nanoparticles, eco-friendly synthesis and evaluation. Arab J Chem. 2021;14(4):103085. doi: 10.1016/j.arabjc.2021.103085.
25. Briand GG, Burford N. Bismuth compounds and preparations with biological or medicinal relevance. Chem Rev. 1999;99(9):2601-58. doi: 10.1021/cr980425s.
26. Domenico P, Cunha BA, Salo RJ, Straus DC, Hutson JC. Salicylate or bismuth salts enhance opsonophagocytosis of *Klebsiella pneumoniae*. Infection. 1992;20(2):66-72. doi: 10.1007/bf01711065.
27. Gump DW, Nadeau OW, Hendricks GM, Meyer DH. Evidence that bismuth salts reduce invasion of epithelial cells by enteroinvasive bacteria. Med Microbiol Immunol. 1992;181(3):131-43. doi: 10.1007/bf00202053.
28. Bush K. Improving known classes of antibiotics: an optimistic approach for the future. Curr Opin Pharmacol. 2012;12(5):527-34. doi: 10.1016/j.coph.2012.06.003.
29. Fischbach MA. Combination therapies for combating antimicrobial resistance. Curr Opin Microbiol. 2011;14(5):519-23. doi: 10.1016/j.mib.2011.08.003.
30. Badireddy AR, Hernandez-Delgadillo R, Sánchez-Nájera RI, Chellam S, Cabral-Romero C. Synthesis and characterization of lipophilic bismuth dimercaptopropanol nanoparticles and their effects on oral microorganisms growth and biofilm formation. J Nanopart Res. 2014;16(6):2456. doi: 10.1007/s11051-014-2456-5.
31. Vega-Jiménez AL, Almaguer-Flores A, Flores-Castañeda M, Camps E, Uribe-Ramírez M, Aztatzi-Aguilar OG, et al. Bismuth subsalicylate nanoparticles with anaerobic antibacterial activity for dental applications. Nanotechnology. 2017;28(43):435101. doi: 10.1088/1361-6528/aa8838.
32. Perinelli DR, Fagioli L, Campana R, Lam JKW, Baffone W, Palmieri GF, et al. Chitosan-based nanosystems and their exploited antimicrobial activity. Eur J Pharm Sci. 2018;117:8-20. doi: 10.1016/j.ejps.2018.01.046.
33. Subils T, Casabonne C, Balagué C. The inhibitory effect of colloidal bismuth hydroxide gel on *Escherichia coli* O157:H7 and on the activity of Shiga toxins. BMC Res Notes. 2014;7:875. doi: 10.1186/1756-0500-7-875.